Technical Paper

Journal of the Society of
Naval Architects of Korea
Vol. 24, No. 1, March 1987

Extension of Guilloton's Method for the Calculation of Wave-making Resistance and Velocities at the Vicinity of a Ship Hull (2nd Report)

D.K. Lee*

Abstract

The materials to develop a computer-based method for the wave resistance of a ship within the frame of Guilloton's wedge concept are presented in this paper. A systematic reliable procedure to retrieve the linearized hull corresponding to a given real hull form (the so-called inverse transformation) has been devised. The algorithm based on the present materials produces evidently accurate values of the H-functions, and the wave profiles and the wave resistance coefficients in good agreement with the experimental measurements.

Notations

x, y, z : the rectangular coordinates with vertically downward z-axis and the static free surface as the $x-y$ plane

ζ : the isobar undulation from its static level

U : the free stream velocity or equivalently the speed of ship

g : acceleration due to the gravity

Γ : the strength of a wedge, Δ^2/m ($=\tan\theta$), Δ^2 : the second difference of offsets

m : the distance between two neighbouring stations, the length of parabolic part of the vertex line of a rounded wedge (see Fig. 4B)

n : the distance between waterlines, the width of a wedge$=2n$

u : the x-component of the disturbance velocity

a : the z-coordinate of the vertex line of a wedge, used to denote the vertical position of a wedge

K : g/U^2, the wave number

F_n : the Froude number of the ship

η : offsets of a hull

$\eta_{T.L.}, \eta_{O.R.}, \eta_{A.R.}$: offsets of the trial linearized hull, the object real hull and the achieved real hull respectively

p : pressure

1. Introduction

The present paper contains the outcomes of research carried on since the publication of the first report[1] under the same title.

The expressions (cf. Appendix) to calculate the values of the H-function for a rounded wedge are incorporated in the present paper and has been used for the analysis of the wave characteristics of the Wigley's

Manuscripts received: December 29, 1986, Revised Manuscripts received: February 4, 1987
* Member, Dept. of Naval Architecture and Ocean Engineering, University of Ulsan

parabolic model. One reason why Guilloton's method is not widely accepted in the practical applications inspite of its superior accuracy and economics of computation may render to the unavailability of readily usable tables for the function or, equivalently, an algorithm to calculate the function values. As is well known[2], a pair of homologous hull forms is assumed in the application of Guilloton's method; one being what is called the linearized hull for which the calculation is performed and the other being the real hull for which the calculated results hold. Another reason may be attributed to the fact that a systematic procedure to find the linearized hull which is homologous to the given real hull is yet to be devised. Emerson[3] showed a way for this but some improvement seems to be required before it can be incorporated in a computer-based numerical processing.

These two matters are the main objects of the present paper. To provide the algorithm, the expression of the derivative of Michell's potential for a wedge, whether it is a sharp one or a rounded one, is heavily manipulated to make the maximum use of analytical integration. It is unexpected reward that a few aspects of the singular behaviours of a wedge which are hidden in the original expression under the multiple integrals are disclosed in this manipulation. The procedure to find the linearized hull from a given real hull cannot but be an iterative one on view of the nonlinear characteristics of the involved substance which will be apparent in due course. An intuitive simple scheme is introduced in the present paper which has proved to work satisfactorily. The basic strategy is that the difference between the hull achieved from a trial linearized hull and the given real hull should be the correction to the trial linearized hull. The given real hull itself can be used as the initial trial linearized hull in the process.

The present method is restricted to the calculation of the wave-making resistance. The expressions for the disturbance velocity components off the hull surface are more opposing to analytic integration, although they appear to be more submissive to numerical integration, than the expression for the wave elevation on the hull surface is. This problem will take some more time and efforts.

Some awkwardness might be felt if one wishes to apply the present method to the design of a hull with curved bow and stern profile because the nose of a wedge is a vertical line. Increase of the number of wedge layers may sufficiently overcome this deficiency. However, the existence of a large bulb creates a real trouble since superposition of wedges cannot adequately represent a bulb-shaped volume on account of the intrinsic geometical property of a wedge.

2. Evaluation of the wedge function

The disturbance velocity created by a wedge is fully described in the reference[1]. Within the scope of the linear theory, only the longitudinal component,

Table 1A The values of $1,000H/n^2$ for a rounded full wedge

position of the wedge $a=n$
position of the calculation $z=2n$

		m													
		0.5					1.0				1.5			2.0	
n	methods \ x	0.25	0.5	1.0	1.5	2.0	0.5	1.0	1.5	2.0	0.75	1.5	2.0	1.0	2.0
0.1	Guilloton	387	296	414	465	450	356	399	465	450	388	441	450	412	416
	present	378	313	429	481	458	376	420	472	453	406	456	444	424	431
0.5	Guilloton	206	171	156	165	176	182	158	166	176	174	166	176	172	173
	present	205	176	163	171	181	185	165	171	180	178	171	179	178	177
1.0	Guilloton	133	117	98	95	95	118	106	97	97	112	100	99	111	100
	prfsent	131	121	109	104	102	122	110	104	102	117	105	102	113	102

Table 1B The values of $1,000H/n^2$ for a rounded half wedge

position of the wedge $a=0$

position of the calculation $z=0$

		m														
		0.5			1.0			1.5			2.0			2.5		
n	methods \ x	0	0.25	0.5	0	0.5	1.0	0	0.75	1.5	0	1.0	2.0	0	1.25	2.5
0.1	Guilloton	278	606	659	321	582	457	321	507	318	306	443	240	287	394	189
	present	270	592	635	312	565	446	309	495	317	296	434	239	278	386	188
0.4	Guilloton	128	278	352	158	325	340	173	317	289	175	307	237	178	285	191
	present	128	277	354	156	321	344	170	321	292	175	307	240	176	287	195
0.8	Guilloton	92	182	245	111	224	268	120	248	245	129	239	213	132	230	179
	present	95	188	246	113	227	267	124	240	248	130	239	218	133	232	185

regardless of the other two, of this disturbance velocity induced at points on the hull surface is necessary for the calculation of the wavemaking resistance or the isobar curve.

In connection with the associated isobar undulation, Guilloton defined H-function of a wedge as the following equation shows.

$$\zeta=2\frac{U^2}{g}\Gamma\frac{H}{n} \qquad (1)$$

or equivalently $u=2U\Gamma\frac{H}{n}$ (2)

The function H consists of one double and two single integrals. The double integral as it would appear by the expressions in the reference[1] is not a convenient form for numerical integration. The two infinite upper limits and the disguised singularity, in some cases, of the integrand can be pointed out as the reasons. An actual application of a quadrature quite strikingly reveals numerical unsteadiness which is obviously related to these reasons. It is desirable therefore to change this integral to a more convenient and less

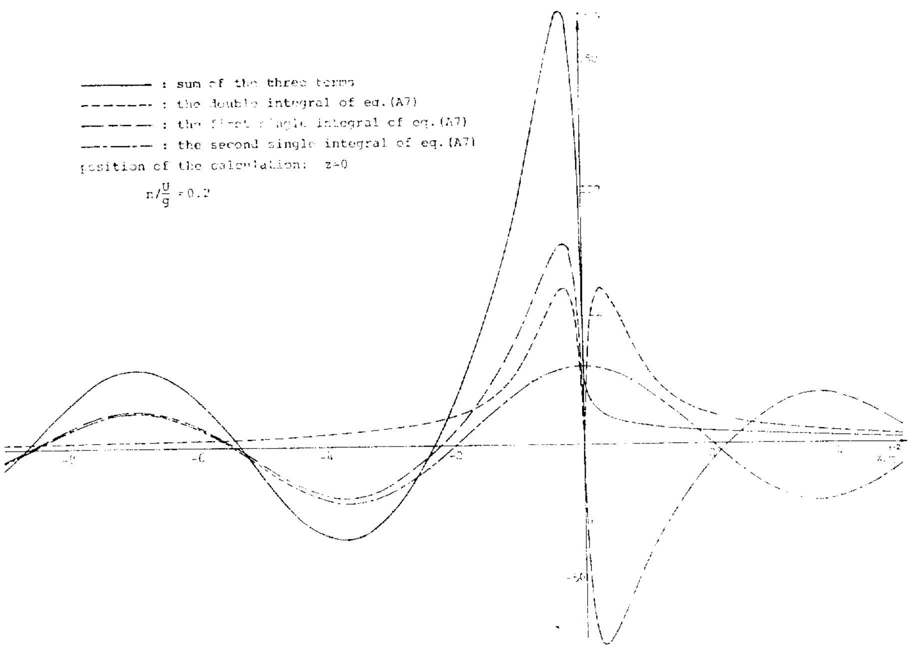

Fig. 1 Example of H/n curve of a sharp full wedge

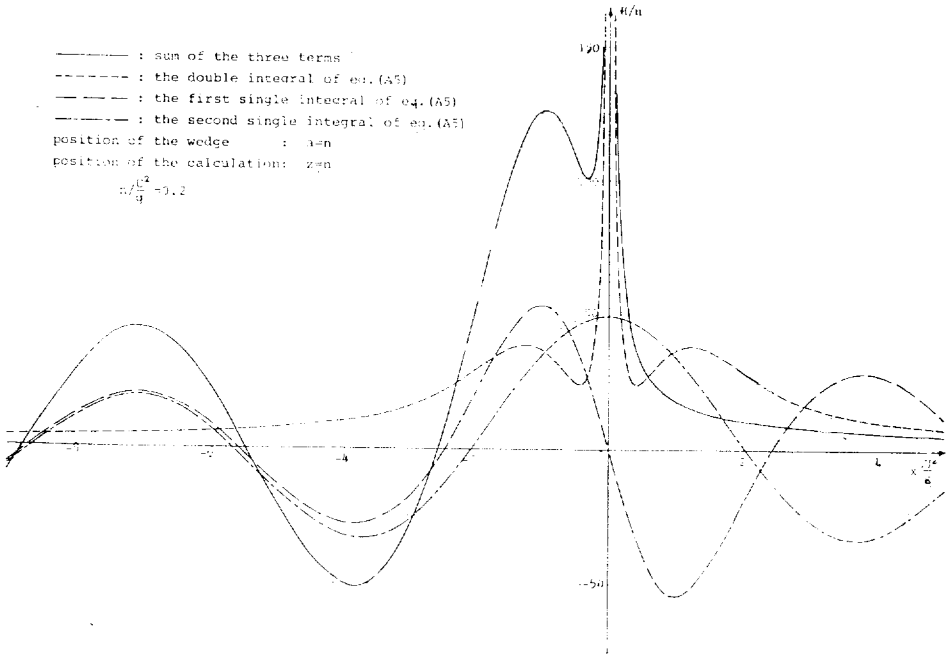

Fig. 2 Example of *H/n* curve of a sharp half wedge

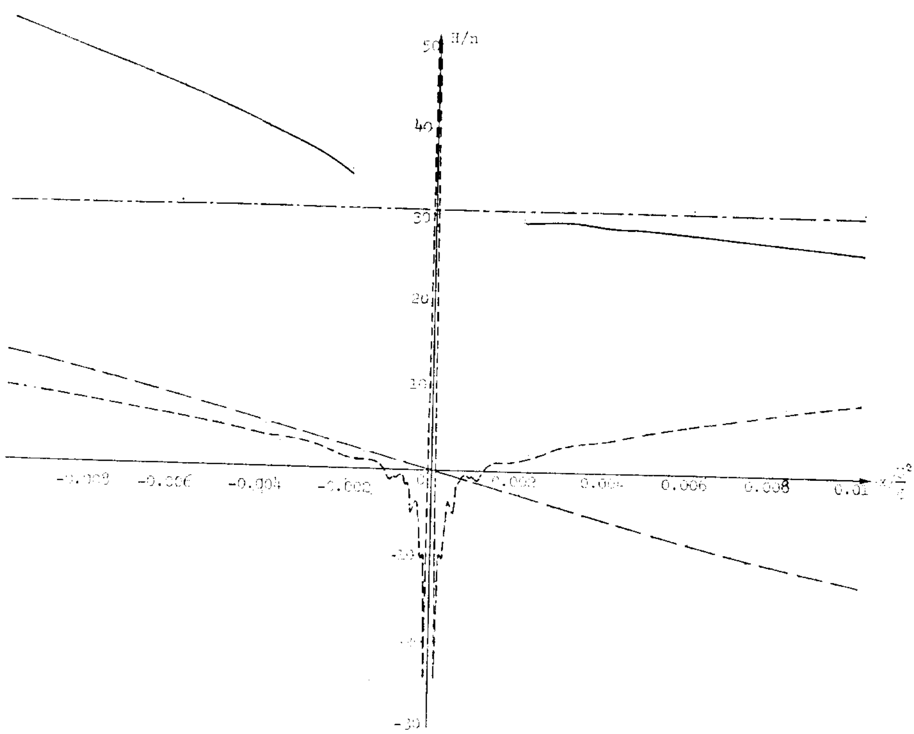

Fig. 3 Enlarged view of the neighbourhood of the origin of the Fig. 2

error-inducing form for the numerical integration, singling out the singularities, if any, at the same time. The details can be found in the Appendix. It can be noticed that a logarithmic singularity does exist when the point of calculation lies on the nose line of a sharp wedge. This is in fact an expected result because it is a well-known fact that the velocity of an ideal fluid becomes infinite at a place where the stream meets a solid boundary whose tangent has a non-zero angle with the direction of the stream. Even in the case of a rounded wedge, the integrand itself diverges when the point of calculation lies on the nose line, although the integral can have a finite value. This means that the position of an isobar at the both ends of a model where sharp wedges are to be placed cannot be determined by the wedge method. However, in reality, this fact may be taken without so great pessimism since, as can be noticed from Fig. 1, 2 and 3, the divergence of the double integral occurs within quite narrow, in the case of a sharp full wedge, and extremely narrow, in the case of a sharp half wedge, neighbourhood of the origin. If necessary, employment of interpolation technics can be a good remedy for a sharp full wedge. In the case of a sharp half wedge, Fig. 3 shows that it is reasonable for practical purposes to ignore the rapid oscillation and to take zero as its value at the origin.

Some examples of the values of H-function obtained by the present method are shown in Table 1 together with Guilloton's own values[4] for comparison.

3. Wedge system and superposition

3.1. The Guilloton model

To evaluate the values of Michell potential, the wave number K should be fixed. Guilloton chose 2.5m for U^2/g $(=K^{-1})$ in developing his wedge method. The length of the model presumed in the process of analysis is then

$$L_G=\frac{2.5}{F_n^2} \qquad [\mathrm{m}]$$

to maintain the identity of the Froude number. The geosim model determined in this way will be referred to by 'the Guilloton model.'

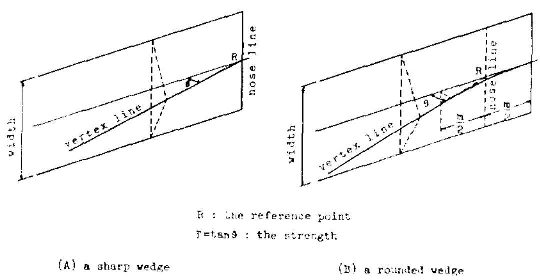

Fig. 4 The notations of wedge

3.2. The wedge system

The Guilloton model is to be represented by the superposition of a number of wedges. It is convenient to place these wedges at the junctions of equally spaced waterlines and stations except those to be placed at the bow and the stern. The details of how an arbitrary hull form is decomposed into the wedge system can be found in the reference [1]. The position of a wedge is referred to by the coordinates of the reference point of the wedge, this being the point where the straight part of the vertex line meets the flat base surface. The terminologies and parameters concerned with wedges are shown in Fig. 4.

3.3. The superposition

The isobar elevation at the reference point (x_i, z_i) of the i-th wedge due to the j-th wedge will be

$$\zeta_{ij}=2\frac{U^2}{g}\Gamma_j\frac{H_{ij}}{n_j} \tag{4}$$

where $H_{ij}\equiv H(x_i, z_i;\ x_j, z_j)$ (5)

(x_j, z_j) being the coordinates of the reference point of the j-th wedge. Then, the isobar elevation due to the whole wedge system to represent the model can be obtained by superposition as follows

$$\zeta(x_i, z_i)=2\frac{U^2}{g}\sum_{j=1}^{N}\Gamma_j H_{ij}/n_j \tag{6}$$

Normally the width of wedge is the same for all the wedges. If this is so, n_j can come out of the summation symbol in the above expression and H_{ij} alone is what may be called the influence coefficient.

4. Hull form transformations

4.1. The transformation

Guilloton argues that the isobar obtained by eq. (6)

is valid not for the real hull but for what is called the linearized hull because the influence coefficients are evaluated by the formula of the linearized theory. He proposes the following transformation to achieve the real hull for which the calculated results are thought to be valid: at a waterline $z=a$

(a) the longitudinal variation

$$x=\int_0^{x_0}\frac{\left[1-\frac{2}{U^2/g}\zeta(x_0,a)\right]^{1/2}}{1+\frac{1}{2}\left(\frac{\partial\eta_0}{\partial x_0}\right)^2}dx_0 \qquad (7)$$

(b) the lateral variation

$$\eta[x,a-\zeta(x_0,a)]=\eta_0(x_0,a) \qquad (8)$$

The two corresponding points, one (x_0,η_0,a) representing the linearized hull and the other $(x,\eta,a-\zeta)$ representing the real hull, are referred to the homologous points. This transformation of the hull form brings in the following effects

(a) on the isobar curves;

$\zeta(x,a)=\zeta_0(x_0,a)$ that is, the phase shift

(b) on the offsets of the hull;

contact of the hull surface with the isobar.

The above process to achieve the real hull from a linearized hull is referred to by the forward transformation or just the transformation. It is to be noted that not only the offsets but the length of the model change by this transformation.

4.2. The inverse transformation

Since the results calculated for a linearized hull are applicable to the real hull achieved by the transformation just described, and the hydrodynamic characteristics of this real hull is actually the matter of interests, a process to find the linearized hull corresponding to a given real hull is of an absolute necessity. This process is what is denoted the inverse transformation. Unlike the forward transformation, this is inevitably to be an iterative process such as Emerson's trial-and-error method[3].

The process devised in the present paper for the inverse transformation can be summarized as the following:

(1) Assume a trial linearized hull.
 * The object real hull may be the natural choice for the initial trial linearized hull.
 * For the consecutive iterations, this is determined at the stage(7).

(2) Construct the influence coefficients matrix.

(3) Calculate the wedge strengths.

(4) Determine the isobar curve by the eq. (6) at each waterline.

(5) Find the real hull implied by this trial linearized hull.
 * This step is the forward transformation.

(6) Compare this achieved real hull with the object real hull.

(7) If the difference is too great, find the new trial linearized hull by
 * the offsets

$$(\eta_{T.L.})_{i+1}=(\eta_{T.L.})_i+[\eta_{O.R.}-(\eta_{A.R.})_i] \qquad (9)$$

 * the length

$$(L_{T.L.})_{i+1}=(L_{T.L.})_i+[L_{O.R.}-(L_{A.R.})_i] \qquad (10)$$

The quantities in the brackets in eq. (9) and (10) are corrections for the next iterative step. As a conservative policy, only so many percent of the required correction may actually be made. This policy can help the convergence. As the Froude number becomes higher, the experiences show that less proportion of the correction is desirable.

5. The wave-making resistance

The wave-making resistance of the model is calculated by integrating the force due to pressure on the longitudinal projection of the model as the following equation shows.

$$R_w=2\int_0^B\left[\left(\int_{-\zeta_{F.B.}}^{z_t}pdz\right)_{\text{ForeBody}}-\left(\int_{-\zeta_{A.B.}}^{z_t}pdz\right)_{\text{Aft Body}}\right]dy$$
$$=2\int_0^B\int_0^{p(z_t)}(\zeta_{F.B.}-\zeta_{A.B.})dpdy \qquad (11)$$

This inegration should be performed on the achieved real hull. In the process of integration, the keel may be assumed to be identical for both the linearized hull and the real hull, and, in addition to be an isobar.

6. The results and comparisons

Wigley's parabolic model used by Emerson[3], and Shearer and Cross[5] has been chosen as a test case

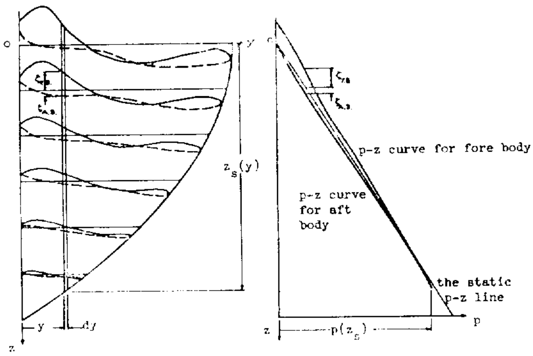

Fig. 5 Calculation of the wave-making resistance

of the present method, the easy access to the experimental data and the results obtained by other methods being the incentive. This was one of the models selected for the workshop organized by DTNSRDC in 1979[6].

In the process of the analysis, to save the computing time, the elements of the influence coefficient matrix concerned with the sternmost wedges were determined by interpolation than by evaluating the integral in each, except the first, iteration. Because the relative positions of the wedges need not vary from iteration to iteration except those in connection with the sternmost wedges, the other elements remain unaltered. This means that every column and every row corresponding to a sternmost wedge of the matrix should be replaced by new values in a new iterative step. Let H_{mn} be taken as an example in which m denotes a non-sternmost wedge and n a sternmost wedge. Since the shape of the isobar curve created by the n-th wedge on the waterline where the m-th wedge lies does not change although the longitudinal position of the m-th wedge relative to the n-th wedge varies everytime in the iteration, it is possible to evaluate H_{mn} by interpolation in each iteration from the isobar curve determined once for all.

More iterations were needed as the Froude number increased to find the linearized hull which would produce the achieved real hull that was within a pre-specified error range from the given real hull. This error range was defined as the ratio of the maximum difference of offsets between the achieved hull and the given hull at the same position to the beam of the given hull. A typical value was 10^{-5}.

At the final step as well as during the iteration, the positions of the sternmost wedges do not make the same profile as the stern of the given hull. Furthermore the length of the corresponding linearized hull, assuming that it is defined in a reasonable manner, would be different from that of the given real hull. This fact raises a question about what space the Froude number identity must be conformed to in. Depending on the choice a different set of results would be obtained. This dilemma is inevitable once we accept Guilloton's space transformation to which merits of the method are believed to owe. In this paper the Froude number identity is assumed to be observed in the real space without any rational but the practical reason that if the Froude number is to be defined in the linearized space the influence coefficient matrix has to be re-constructed in each iteration which will make the problem too much entangled.

Some difficulties have been experienced in the nu-

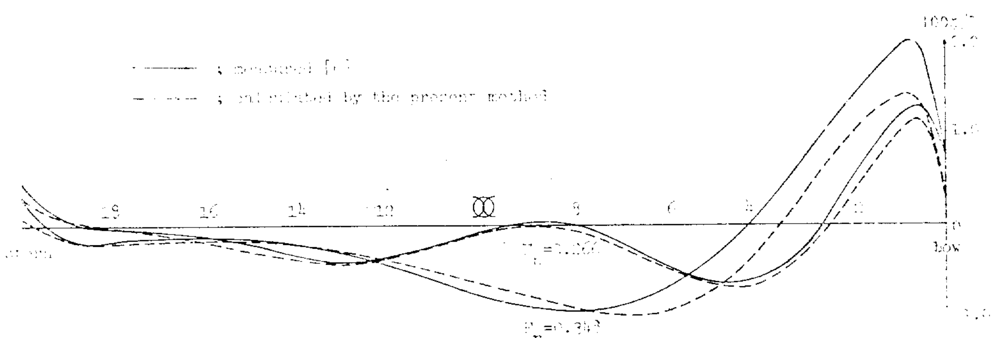

Fig. 6 Wave elevation of Wigley's parabolic model projected to the

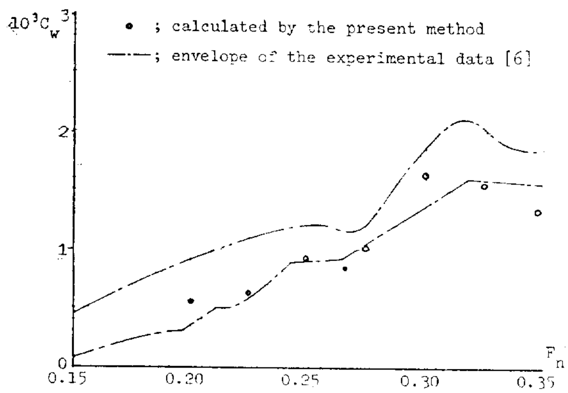

Fig. 7 Wave-making resistance coeffiicients of Wigley's parabolic model

merical integration of ζ-curve with respect to pressure (eq. 11) on account of the fact that the y-coordinates following the ζ-curve on the body plan are not always in sequential order. Some errors on the wave-making resistance are included in the present results on this account.

The calculated results are presented in the forms of the surface wave elevation (Fig. 6) and the wave-making resistance coefficients (Fig. 7). The calculated wave elevation is in good agreement with the measured one. This agreement was better with decreasing Froude number. The most prominent discrepancy however appears at the neighbourhood of the bow. This was observed to be a general trend. It is believed that this discrepancy has some relation with the singular behaviour of the integrand described previously and might be improved in that connection.

The calculated wave-making resistance coefficients show a general tendency that the present method predicts a low wave-making resistance. Although the overall assesment may be summarized as excellent there are places not totally satisfactory. This must be attributed to the unsatisfactory numberical integration of the pressure curve rather than to the intrinsic property of the method. It was felt to be certain that, with an improved capability of the interpolation routine, more accurate values of the resistance coefficient can be obtained.

References

〔1〕 Lee, D.K., "Extension of Guilloton's Method for the Calculation of Wave-making Resistance and Velocities at the Vicinity of a Ship Hull (1st Report)", *Journal of SNAK*, Vol. 21, No. 3, Sep. 1984, p. 19.

〔2〕 Guilloton, R., "L'étude théorique du bateau en fluide parfait", ***Bulletin ATMA***, No. 64, 1964, p. 537.

〔3〕 Emerson, A., "The calculation of ship resistance: an application of Guilloton's method", ***Trans.*** *RINA*, Vol. 109, 1967, p. 241.

〔4〕 Guilloton, R., "Potential theory of wave resistance of ships with tables for its calculation", ***Trans.*** *SNAME*, Vol. 59, 1951, p. 86.

〔5〕 Shearer, J.R. and Cross, J.J., "The experimental determination of the components of ship resistance for a mathematical model", *Trans. RINA*, Vol. 107, 1965, p. 459.

〔6〕 Bai, K.J. and McCarthy, J.H., Proceedings of the workshop on ship wave-resistance computations", DTNSRDC, Nov. 1979.

Appendix

It can be seen from the reference[1] that the x-component of the disturbance velocity induced at a point $(x, 0, z)$ by a wedge whose reference point is located at $(x_0, 0, a)$ are, after some arithmetic works, as the following;

(1) the rounded full wedge

$$u(x, 0, z; x_0, 0, a) = 2U\Gamma\frac{1}{n}H(x, z; x_0, a)$$

$$= 2U\Gamma\frac{1}{n}\left\{\frac{4K^2}{\pi^2 m}\int_0^\infty\int_0^\infty\frac{e^{-y\sqrt{\sigma^2+\tau^2}}[1-\cos(n\tau)]}{\sigma\sqrt{\sigma^2+\tau^2}\,(\sigma^4+K^2\tau^2)}\left[\cos(\tau z)-\frac{\sigma^2}{K\tau}\sin(\tau z)\right]\left[\cos(a\tau)\right.\right.$$

$$
\begin{aligned}
&-\frac{\sigma^2}{K\tau}\sin(a\tau)\Big]\cos[\sigma(x-x_0)]\sin\frac{m\sigma}{2}\,d\sigma d\tau-\frac{2}{\pi mK^2}\int_0^{\pi/2}e^{-K(z+a)\sec^2\alpha}(e^{-Kn\sec^2\alpha}\\
&-2+e^{Kn\sec^2\alpha})\sin[K(x-x_0)\sec\alpha]\sin\left(\frac{Km}{2}\sec\alpha\right)\cos^3\alpha\,d\alpha+\frac{2}{\pi mK^2}\int_0^{\pi/2}e^{-K(z+a)\cos^2\alpha}(e^{-Kn\cos^2\alpha}\\
&-2+e^{Kn\cos^2\alpha})\cos[K(x-x_0)\cos\alpha]\sin\left(\frac{Km}{2}\cos\alpha\right)\sec^4\alpha\,d\alpha\Big\}_{y=0} \qquad \text{(A1)}
\end{aligned}
$$

The expression within the curly brackets is the Guilloton's H-function for a rounded full wedge. The double integral can be changed to the form shown below (writing x instead of $x-x_0$ which is equivalent to taking the origin of the local coordinate system at the intersection of the vertical line passing through the reference point of the wedge and the calm free surface);

$$
\begin{aligned}
&\left\{\int_0^\infty\int_0^\infty\frac{e^{-y\sqrt{\sigma^2+\tau^2}}[1-\cos(n\tau)]}{\sigma\sqrt{\sigma^2+\tau^2}(\sigma^4+K^2\tau^2)}\left[\cos(\tau z)-\frac{\sigma^2}{K\tau}\sin(\tau z)\right]\left[\cos(a\tau)-\frac{\sigma^2}{K\tau}\sin(a\tau)\right]\cos(\sigma x)\sin\frac{m\sigma}{2}\,d\sigma d\tau\right\}_{y=0}\\
&=-\frac{\pi}{16K^2}\int_{-m/2}^{m/2}\Big\{(z+a)\Big[\sinh^{-1}\frac{n[2(z+a)+n]}{(z+a+n)\sqrt{(|x|+\mu)^2+(z+a)^2}+(z+a)\sqrt{(|x|+\mu)^2+(z+a+n)^2}}\\
&\quad-\sinh^{-1}\frac{n[2(z+a)-n]}{(z+a)\sqrt{(|x|+\mu)^2+(z+a-n)^2}+(z+a-n)\sqrt{(|x|+\mu)^2+(z+a)^2}}\Big]\\
&\quad+n\Big[\sinh^{-1}\frac{4n(z+a)}{(z+a+n)\sqrt{(|x|+\mu)^2+(z+a-n)^2}+(z+a-n)\sqrt{(|x|+\mu)^2+(z+a+n)^2}}\\
&\quad-\sinh^{-1}\frac{(z-a+n)\sqrt{(|x|+\mu)^2+(z-a-n)^2}-(z-a-n)\sqrt{(|x|+\mu)^2+(z-a+n)^2}}{(|x|+\mu)^2}\Big]\\
&\quad-(z-a)\Big[\sinh^{-1}\frac{(z-a+n)\sqrt{(|x|+\mu)^2+(z-a)^2}-(z-a)\sqrt{(|x|+\mu)^2+(z-a+n)^2}}{(|x|+\mu)^2}\\
&\quad-\sinh^{-1}\frac{(z-a)\sqrt{(|x|+\mu)^2+(z-a-n)^2}-(z-a-n)\sqrt{(|x|+\mu)^2+(z-a)^2}}{(|x|+\mu)^2}\Big]\Big\}d\mu\\
&+\frac{\pi}{32K^2}\Big\{\left(|x|+\frac{m}{2}\right)\Big[\sqrt{\left(|x|+\frac{m}{2}\right)^2+(z+a+n)^2}-2\sqrt{\left(|x|+\frac{m}{2}\right)^2+(z+a)^2}+\sqrt{\left(|x|+\frac{m}{2}\right)^2+(z+a-n)^2}\\
&\quad-\sqrt{\left(|x|+\frac{m}{2}\right)^2+(z-a+n)^2}+2\sqrt{\left(|x|+\frac{m}{2}\right)^2+(z-a)^2}-\sqrt{\left(|x|+\frac{m}{2}\right)^2+(z-a-n)^2}\Big]\\
&\quad-\left(|x|-\frac{m}{2}\right)\Big[\sqrt{\left(|x|-\frac{m}{2}\right)^2+(z+a+n)^2}-2\sqrt{\left(|x|-\frac{m}{2}\right)^2+(z+a)^2}+\sqrt{\left(|x|-\frac{m}{2}\right)^2+(z+a-n)^2}\\
&\quad-\sqrt{\left(|x|-\frac{m}{2}\right)^2+(z-a+n)^2}+2\sqrt{\left(|x|-\frac{m}{2}\right)^2+(z-a)^2}-\sqrt{\left(|x|-\frac{m}{2}\right)^2+(z-a-n)^2}\Big]\\
&\quad+(z+a+n)^2\sinh^{-1}\frac{\left(|x|+\frac{m}{2}\right)\sqrt{\left(|x|-\frac{m}{2}\right)^2+(z+a+n)^2}-\left(|x|-\frac{m}{2}\right)\sqrt{\left(|x|+\frac{m}{2}\right)^2+(z+a+n)^2}}{(z+a+n)^2}\\
&\quad-2(z+a)^2\sinh^{-1}\frac{\left(|x|+\frac{m}{2}\right)\sqrt{\left(|x|-\frac{m}{2}\right)^2+(z+a)^2}-\left(|x|-\frac{m}{2}\right)\sqrt{\left(|x|+\frac{m}{2}\right)^2+(z+a)^2}}{(z+a)^2}\\
&\quad+(z+a-n)^2\sinh^{-1}\frac{\left(|x|+\frac{m}{2}\right)\sqrt{\left(|x|-\frac{m}{2}\right)^2+(z+a-n)^2}-\left(|x|-\frac{m}{2}\right)\sqrt{\left(|x|+\frac{m}{2}\right)^2+(z+a-n)^2}}{(z+a-n)^2}\\
&\quad-(z-a+n)^2\sinh^{-1}\frac{\left(|x|+\frac{m}{2}\right)\sqrt{\left(|x|-\frac{m}{2}\right)^2+(z-a+n)^2}-\left(|x|-\frac{m}{2}\right)\sqrt{\left(|x|+\frac{m}{2}\right)^2+(z-a+n)^2}}{(z-a+n)^2}\\
&\quad+2(z-a)^2\sinh^{-1}\frac{\left(|x|+\frac{m}{2}\right)\sqrt{\left(|x|-\frac{m}{2}\right)^2+(z-a)^2}-\left(|x|-\frac{m}{2}\right)\sqrt{\left(|x|+\frac{m}{2}\right)^2+(z-a)^2}}{(z-a)^2}\\
&\quad-(z-a-n)^2\sinh^{-1}\frac{\left(|x|+\frac{m}{2}\right)\sqrt{\left(|x|-\frac{m}{2}\right)^2+(z-a-n)^2}-\left(|x|-\frac{m}{2}\right)\sqrt{\left(|x|+\frac{m}{2}\right)^2+(z-a-n)^2}}{(z-a-n)^2}\Big\}
\end{aligned}
$$

$$+\frac{\pi}{8K^3}\left\{\int_0^n\left[\int_0^{u_1}\frac{e^{-K\omega e_4}-e^{-K\omega e_2}}{\omega^2\sqrt{1+\omega^2}}d\omega+\int_{u_1}^{u_2}\frac{e^{-K\omega e_4}-1}{\omega^2\sqrt{1+\omega^2}}d\omega\right]d\nu-\mathrm{sign}\left(|x|-\frac{m}{2}\right)\right.$$

$$\left.\int_0^n\left[\int_0^{u_3}\frac{e^{-K\omega e_8}-e^{-K\omega e_6}}{\omega^2\sqrt{1+\omega^2}}d\omega+\int_{u_3}^{u_4}\frac{e^{-K\omega e_8}-1}{\omega^2\sqrt{1+\omega^2}}d\omega\right]d\nu\right\}$$

$$+\frac{\pi}{8K^2}\int_0^n\left\{\left(|x|+\frac{m}{2}\right)\ln\frac{(z+a+\nu)(1+\sqrt{1+u_1^2})}{(z+a-\nu)(1+\sqrt{1+u_2^2})}+\left(|x|-\frac{m}{2}\right)\ln\frac{(z+a-\nu)(1+\sqrt{1+u_4^2})}{(z+a+\nu)(1+\sqrt{1+u_3^2})}\right.$$

$$+\begin{cases}(z+a+\nu)\ln\dfrac{|x|+\frac{m}{2}+(z+a+\nu)\sqrt{1+u_1^2}}{\left||x|-\frac{m}{2}\right|+(z+a+\nu)\sqrt{1+u_3^2}}+(z+a-\nu)\ln\dfrac{\left||x|-\frac{m}{2}\right|+(z+a-\nu)\sqrt{1+u_4^2}}{|x|+\frac{m}{2}+(z+a-\nu)\sqrt{1+u_2^2}} & \text{when } |x|>\frac{m}{2}\\[2ex] (z+a+\nu)\ln\dfrac{\left[|x|+\frac{m}{2}+(z+a+\nu)\sqrt{1+u_1^2}\right]\left[\left||x|-\frac{m}{2}\right|+(z+a+\nu\sqrt{1+u_3^2}\right]}{(z+a+\nu)^2} \\ \quad-(z+a-\nu)\ln\dfrac{\left[|x|+\frac{m}{2}+(z+a-\nu)\sqrt{1+u_2^2}\right]\left[\left||x|-\frac{m}{2}\right|+(z+a-\nu)\sqrt{1+u_4^2}\right]}{(z+a-\nu)^2} & \text{when } |x|<\frac{m}{2}\end{cases}\left.\vphantom{\int}\right\}d\nu \quad \text{(A2)}$$

with the notations;

$$u_1=\left(|x|+\frac{m}{2}\right)/(z+a+\nu)\quad u_2=\left(|x|+\frac{m}{2}\right)/(z+a-\nu)\quad u_3=\left||x|-\frac{m}{2}\right|/(z+a+\nu)\quad u_4=\left||x|-\frac{m}{2}\right|/(z+a-\nu)$$

$$e_1=|x|+\frac{m}{2}+\omega(z+a+\nu)\quad e_2=|x|+\frac{m}{2}-\omega(z+a+\nu)\quad e_3=|x|+\frac{m}{2}+\omega(z+a-\nu)\quad e_4=|x|+\frac{m}{2}-\omega(z+a-\nu)$$

$$e_5=\left||x|-\frac{m}{2}\right|+\omega(z+a+\nu)\quad e_6=\left||x|-\frac{m}{2}\right|-\omega(z+a+\nu)\quad e_7=\left||x|-\frac{m}{2}\right|+\omega(z+a-\nu)\quad e_8=\left||x|-\frac{m}{2}\right|-\omega(z+a-\nu)$$

The integrand of the first term as $(|x|+\mu)\to 0$ is

(a) when $z>a+n$ or $0<z<a-n$

$$(z+a)\left[\sinh^{-1}\frac{n\left(z+a+\frac{n}{2}\right)}{(z+a)(z+a+n)}-\sinh^{-1}\frac{n\left(z+a-\frac{n}{2}\right)}{(z+a)(z+a-n)}\right]+n\sinh^{-1}\frac{2n(z+a)}{(z+a)^2-n^2}$$

$$-|z-a|\left[\sinh^{-1}\frac{n\left(|z-a|+\frac{n}{2}\right)}{|z-a|(|z-a|+n)}-\sinh^{-1}\frac{n\left(|z-a|-\frac{n}{2}\right)}{|z-a|(|z-a|-n)}-n\sinh^{-1}\frac{2n|z-a|}{(z-a)^2-n^2}\right.$$

(b) when $a-n\leq z\leq a+n$

$$(z+a)\left[\sinh^{-1}\frac{n\left(z+a+\frac{n}{2}\right)}{(z+a)(z+a+n)}-\sinh^{-1}\frac{n\left(z+a-\frac{n}{2}\right)}{(z+a)(z+a-n)}+n\sinh^{-1}\frac{2n(z+a)}{(z+a)^2-n^2}\right.$$

$$-|z-a|\sinh^{-1}\frac{n\left(|z-a|+\frac{n}{2}\right)}{|z-a|(|z-a|+n)}+|z-a|\ln 4|z-a|-n\ln 4(n+|z-a|)-(n-|z-a|)\ln(n-|z-a|)$$

$$+(n-|z-a|)\ln(|x|+\mu)^2$$

with the understanding that $\lim_{\epsilon\to 0}\epsilon\sinh^{-1}\frac{1}{\epsilon}=0$ and $\lim_{\epsilon\to 0}\epsilon\ln\epsilon=0$.

(2) the rounded half wedge

$$u(x,0,z;x_0,0,0)=2U\Gamma\frac{1}{n}H(x,z;x_0,0)$$

$$=2U\Gamma\frac{1}{n}\left\{\frac{2K^2}{\pi^2 m}\int_0^\infty\int_0^\infty\frac{\sigma e^{-y\sqrt{\sigma^2+\tau^2}}}{\sqrt{\sigma^2+\tau^2}(\sigma^4+K^2\tau^2)}\left[\cos(\tau z)-\frac{\sigma^2}{K\tau}\sin(\tau z)\right]\left[\frac{1-\cos(n\tau)}{\sigma^2}\right.\right.$$

$$\left.-\frac{n\tau-\sin(n\tau)}{K\tau}\right]\cos[\sigma(x-x_0)]\sin\frac{m\sigma}{2}d\sigma d\tau$$

$$-\frac{2}{\pi m K^2}\int_0^{\pi/2}e^{-Kz\sec^2\alpha}(e^{-Kn\sec^2\alpha}+Kn\sec^2\alpha-1)\sin[K(x-x_0)\sec\alpha]\sin\left(\frac{Km}{2}\sec\alpha\right)\cos^3\alpha\, d\alpha$$

$$\left.+\frac{2}{\pi m K^2}\int_0^{\pi/2}e^{-Kz\cos^2\alpha}(e^{-Kn\cos^2\alpha}+Kn\cos^2\alpha-1)\cos[K(x-x_0)\cos\alpha]\sin\left(\frac{Km}{2}\cos\alpha\right)\sec^4\alpha d\alpha\right\}_{y=0}\quad \text{(A3)}$$

The double integral can be changed, with the same arrangement as the previous case, to the following form;

$$\left\{\int_0^\infty\int_0^\infty \frac{\sigma e^{-y\sqrt{\sigma^2+\tau^2}}}{\sqrt{\sigma^2+\tau^2}(\sigma^4+K^2\tau^2)}\left[\cos(\tau z)-\frac{\sigma^2}{K\tau}\sin(\tau z)\right]\left[\frac{1-\cos(n\tau)}{\sigma^2}-\frac{n\tau-\sin(n\tau)}{K\tau}\right]\cos(\sigma x)\sin\frac{m\sigma}{2}d\sigma d\tau\right\}_{y=0}$$

$$=\frac{\pi}{16K^3}\left\{\left(|x|+\frac{m}{2}\right)\left[\frac{\sqrt{1+v_1^2}}{v_1^2}-\mathrm{csch}^{-1}v_1-\frac{z-n}{|z-n|}\left(\frac{\sqrt{1+v_2^2}}{v_2^2}-\mathrm{csch}^{-1}v_2\right)\right]\right.$$

$$-\left.\left(|x|-\frac{m}{2}\right)\left[\frac{\sqrt{1+v_3^2}}{v_3^2}-\mathrm{csch}^{-1}v_3-\frac{z-n}{|z-n|}\left(\frac{\sqrt{1+v_4^2}}{v_4^2}-\mathrm{csch}^{-1}v_4\right)\right]\right\}$$

$$+\frac{\pi}{8K^3}\int_0^n\left[K(z+\nu)\sinh^{-1}u_1-K(z-\nu)\sinh^{-1}u_2+K\left(|x|+\frac{m}{2}\right)\left(\mathrm{csch}^{-1}u_1-\frac{z-\nu}{|z-\nu|}\mathrm{csch}^{-1}u_2\right)\right.$$

$$\left.-\int_0^{u_1}\frac{e^{-K\omega e_1}-e^{-K\omega e_2}}{\omega^2\sqrt{1+\omega^2}}d\omega-\int_{u_1}^{u_2}\frac{1-e^{-K\omega e_2}}{\omega^2\sqrt{1+\omega^2}}d\omega-H(\nu-z)\int_{u_2}^\infty\frac{e^{K\omega^2(z-\nu)}(e^{2K\omega(|x|+m/2)}-1)}{\omega^2\sqrt{1+\omega^2}e^{K\omega(|x|+m/2)}}d\omega\right]d\nu$$

$$+\frac{\pi}{8K^4}\left\{\int_0^{v_1}\frac{e^{-K\omega\gamma_2}-e^{-K\omega\gamma_1}+2Kn\omega^2e^{-K\omega\gamma_5}}{\omega^4\sqrt{1+\omega^2}}d\omega+\int_{v_1}^{v_2}\frac{e^{-K\omega\gamma_2}-K(z-n)\omega^2-1}{\omega^4\sqrt{1+\omega^2}}d\omega\right.$$

$$\left.-H(n-z)\int_{v_2}^\infty\frac{e^{K\omega^2(z-n)}[e^{2K\omega(|x|+m/2)}-1]}{\omega^4\sqrt{1+\omega^2}e^{K\omega(|x|+m/2)}}dw+2Kn\int_{v_1}^{v_5}\frac{e^{-K\omega\gamma_5}-1}{\omega^2\sqrt{1+\omega^2}}d\omega\right\}$$

$$-\frac{|x|-\frac{m}{2}}{\left||x|-\frac{m}{2}\right|}\left\{\frac{\pi}{8K^3}\int_0^n\left[K(z+\nu)\sinh^{-1}u_3-K(z-\nu)\sinh^{-1}u_4+K\left||x|-\frac{m}{2}\right|\left(\mathrm{csch}^{-1}u_3-\frac{z-\nu}{|z-\nu|}\mathrm{csch}^{-1}u_4\right)\right.\right.$$

$$\left.-\int_0^{u_3}\frac{e^{-K\omega e_3}-e^{-K\omega e_4}}{\omega^2\sqrt{1+\omega^2}}d\omega-\int_{u_3}^{u_4}\frac{1-e^{-K\omega e_4}}{\omega^2\sqrt{1+\omega^2}}d\omega-H(\nu-z)\int_{u_4}^\infty\frac{e^{K\omega^2(z-\nu)}(e^{2K\omega||x|-m/2|}-1)}{\omega^2\sqrt{1+\omega^2}e^{K\omega||x|-m/2|}}d\omega\right\}d\nu$$

$$+\frac{\pi}{8K^4}\left[\int_0^{v_3}\frac{e^{-K\omega\gamma_4}-e^{-K\omega\gamma_3}+2Kn\omega^2e^{-K\omega\gamma_6}}{w^4\sqrt{1+\omega^2}}d\omega+\int_{v_3}^{v_4}\frac{e^{-K\omega\gamma_4}-K(z-n)\omega^2-1}{\omega^4\sqrt{1+\omega^2}}d\omega\right.$$

$$\left.\left.-H(n-z)\int_{v_4}^\infty\frac{e^{K\omega^2(z-n)}(e^{2K\omega||x|-m/2|}-1)}{\omega^4\sqrt{1+\omega^2}e^{K\omega||x|-m/2|}}d\omega+2Kn\int_{v_3}^{v_6}\frac{e^{-K\omega\gamma_6}-1}{\omega^2\sqrt{1+\omega^2}}d\omega\right]\right\}\tag{A4}$$

with the notations;

$u_1=\left(|x|+\frac{m}{2}\right)/(z+\nu)$ $u_2=\left(|x|+\frac{m}{2}\right)/|z-\nu|$ $u_3=\left||x|-\frac{m}{2}\right|/(z+\nu)$ $u_4=\left||x|-\frac{m}{2}\right|/|z-\nu|$

$v_1=\left(|x|+\frac{m}{2}\right)/(z+n)$ $v_2=\left(|x|+\frac{m}{2}\right)/|z-n|$ $v_3=\left||x|-\frac{m}{2}\right|/(z+n)$ $v_4=\left||x|-\frac{m}{2}\right|/|z-n|$

$v_5=\left(|x|+\frac{m}{2}\right)/z$ $v_6=\left||x|-\frac{m}{2}\right|/z$

$e_1=|x|+\frac{m}{2}-\omega(z+\nu)$ $e_2=|x|+\frac{m}{2}-\omega(z-\nu)$ $e_3=\left||x|-\frac{m}{2}\right|-\omega(z+\nu)$ $e_4=\left||x|-\frac{m}{2}\right|-\omega(z-\nu)$

$\gamma_1=|x|+\frac{m}{2}-\omega(z+n)$ $\gamma_2=|x|+\frac{m}{2}-\omega(z-n)$ $\gamma_3=\left||x|-\frac{m}{2}\right|-\omega(z+n)$ $\gamma_4=\left||x|-\frac{m}{2}\right|-\omega(z-n)$

$\gamma_5=|x|+\frac{m}{2}-\omega z$ $\gamma_6=\left||x|-\frac{m}{2}\right|-\omega z$

(3) the sharp full wedge

$u(x,0,z;x_0,0,a)=2U\Gamma\frac{1}{n}H(x,z;x_0,a)$

$$=2U\Gamma\frac{1}{n}\left\{\frac{2K^2}{\pi^2}\int_0^\infty\int_0^\infty\frac{e^{-y\sqrt{\sigma^2+\tau^2}}[1-\cos(n\tau)]}{\sqrt{\sigma^2+\tau^2}(\sigma^4+K^2\tau^2)}\left[\cos(\tau z)-\frac{\sigma^2}{K\tau}\sin(\tau z)\right]\right.$$

$$\left[\cos(a\tau)-\frac{\sigma^2}{K\tau}\sin(a\tau)\right]\cos[\sigma(x-x_0)]d\sigma d\tau$$

$$-\frac{1}{\pi K}\int_0^{\pi/2}e^{-K(z+a)\sec^2\alpha}(e^{-Kn\sec^2\alpha}-2+e^{Kn\sec^2\alpha})\sin[K(x-x_0)\sec\alpha]\cos^2\alpha\,d\alpha$$

$$\left.+\frac{1}{\pi K}\int_0^{\pi/2}e^{-K(z+a)\cos^2\alpha}(e^{-Kn\cos^2\alpha}-2+e^{Kn\cos^2\alpha})\cos[K(x-x_0)\cos\alpha]\sec^3\alpha d\alpha\right\}_{y=0}\tag{A5}$$

The double integral can be changed to the following form (with x instead of $x-x_0$);

$$\left\{\int_0^\infty\int_0^\infty \frac{e^{-y\sqrt{\sigma^2+\tau^2}}[1-\cos(n\tau)]}{\sqrt{\sigma^2+\tau^2}(\sigma^4+K^2\tau^2)}\left[\cos(\tau z)-\frac{\sigma^2}{K\tau}\sin(\tau z)\right]\left[\cos(a\tau)-\frac{\sigma^2}{K\tau}\sin(a\tau)\right]\cos(\sigma x)\,d\sigma\,d\tau\right\}_{y=0}$$

$$=\frac{\pi}{8K^2}\int_0^n\left\{\ln\frac{[z+a-\nu+\sqrt{x^2+(z+a-\nu)^2}][z-a+\nu+\sqrt{x^2+(z-a+\nu)^2}]}{[z+a+\nu+\sqrt{x^2+(z+a+\nu)^2}][z-a-\nu+\sqrt{x^2+(z-a-\nu)^2}]}\right.$$

$$\left.+2\int_{|x|/(z+a+\nu)}^{|x|/(z+a-\nu)}\frac{1-e^{-K\omega(|x|-\omega(z+a-\nu))}}{\omega\sqrt{1+\omega^2}}d\omega+2\int_0^{|x|/(z+a+\nu)}\frac{e^{K\omega^2\nu}-e^{-K\omega^2\nu}}{\omega\sqrt{1+\omega^2}}e^{-K\omega(|x|-\omega(z+a))}d\omega\right\}d\nu \qquad \text{(A6)}$$

As $x\to 0$, the value of this integral is

(a) when $0\le z\le a-n$ or $z\ge a+n$

$$\frac{\pi}{8K^2}[2(z+a)\ln(z+a)-2|z-a|\ln|z-a|-(z+a+n)\ln(z+a+n)-(z+a-n)\ln(z+a-n)$$
$$+(|z-a|+n)\ln(|z-a|+n)+(|z-a|-n)\ln(|z-a|-n)]$$

(b) when $a-n<z<a+n$

$$\frac{\pi}{8K^2}[2(z+a)\ln(z+a)-2|z-a|\ln|z-a|-(z+a+n)\ln(z+a+n)-(z+a-n)\ln(z+a-n)$$
$$+(a+n-z)\ln(a+n-z)+(z-a+n)\ln(z-a+n)+\lim_{\epsilon\to 0}2(|z-a|-n)(1+\ln\epsilon)]$$

As $|z-a|\to n$, ϵ behaves the same as $|z-a|-n$.

A logarithmic singularity does exist, as expected, in this case.

(4) the sharp half wedge

$$u(x,0,z;x_0,0,0)=2U\Gamma\frac{1}{n}H(x,z;x_0,0)$$

$$=2U\Gamma\frac{1}{n}\left\{\frac{K^2}{\pi^2}\int_0^\infty\int_0^\infty\frac{\sigma^2e^{-y\sqrt{\sigma^2+\tau^2}}}{\sqrt{\sigma^2+\tau^2}(\sigma^4+K^2\tau^2)}\left[\cos(\tau z)-\frac{\sigma^2}{K\tau}\sin(\tau z)\right]\right.$$

$$\left[\frac{1-\cos(n\tau)}{\sigma^2}-\frac{n\tau-\sin(n\tau)}{K\tau}\right]\cos[\sigma(x-x_0)]\,d\sigma\,d\tau$$

$$-\frac{1}{\pi K}\int_0^{\pi/2}e^{-Kz\sec^2\alpha}(e^{-Kn\sec^2\alpha}+Kn\sec^2\alpha-1)\sin[K(x-x_0)\sec\alpha]\cos^2\alpha\,d\alpha$$

$$\left.+\frac{1}{\pi K}\int_0^{\pi/2}e^{-Kz\cos^2\alpha}(e^{-Kn\cos^2\alpha}+Kn\cos^2\alpha-1)\cos[K(x-x_0)\cos\alpha]\sec^3\alpha\,d\alpha\right\}_{y=0} \qquad \text{(A7)}$$

The double integral can be changed to the following form (with x instead of $x-x_0$);

$$\left\{\int_0^\infty\int_0^\infty\frac{\sigma^2e^{-y\sqrt{\sigma^2+\tau^2}}}{\sqrt{\sigma^2+\tau^2}(\sigma^4+K^2\tau^2)}\left[\cos(\tau z)-\frac{\sigma^2}{K\tau}\sin(\tau z)\right]\left[\frac{1-\cos(n\tau)}{\sigma^2}-\frac{n\tau-\sin(n\tau)}{K\tau}\right]\cos(\sigma x)\,d\sigma\,d\tau\right\}_{y=0}$$

$$=\frac{\pi}{8K^2}\int_0^n\left\{\int_0^{u_1}\frac{e^{-K\omega e_2}-e^{-K\omega e_1}}{\omega\sqrt{1+\omega^2}}d\omega-\int_{u_1}^\infty\frac{e^{K\omega e_2}+e^{-K\omega e_1}-2}{\omega\sqrt{1+\omega^2}}d\omega+\text{sign}(z-\nu)\left(\int_0^{u_2}\frac{e^{-K\omega e_3}-e^{-K\omega e_4}}{\omega\sqrt{1+\omega^2}}d\omega\right.\right.$$

$$\left.\left.+\int_{u_2}^\infty\frac{e^{K\omega e_4}+e^{-K\omega e_3}-2}{\omega\sqrt{1+\omega^2}}d\omega\right)\right\}d\nu$$

$$+\frac{\pi}{8K^3}\left\{\int_0^{v_1}\frac{3e^{-K\omega\gamma_2}-e^{-K\omega\gamma_1}-e^{-K\omega\gamma_3}-e^{-K\omega\gamma_4}+2e^{-K\omega\gamma_5}-2e^{-K\omega\gamma_6}-4Kn\omega^2e^{-K\omega\gamma_6}}{\omega^3\sqrt{1+\omega^2}}d\omega\right.$$

$$+\int_{v_1}^{v_2}\frac{e^{-K\omega\gamma_1}+e^{K\omega\gamma_2}-e^{-K\omega\gamma_3}-e^{-K\omega\gamma_4}}{\omega^3\sqrt{1+\omega^2}}d\omega-\int_{v_2}^\infty\frac{e^{K\omega\gamma_2}+e^{K\omega\gamma_4}-2e^{K\omega\gamma_6}+e^{-K\omega\gamma_1}+e^{-K\omega\gamma_3}-2e^{-K\omega\gamma_5}}{\omega^3\sqrt{1+\omega^2}}d\omega$$

$$\left.+2\int_{v_1}^{v_3}\frac{2-e^{K\omega\gamma_2}-e^{-K\omega\gamma_1}+e^{-K\omega\gamma_5}-e^{-K\omega\gamma_6}-2Kn\omega^2e^{-K\omega\gamma_6}}{\omega^3\sqrt{1+\omega^2}}d\omega+2\int_{v_3}^{v_2}\frac{(e^{K\omega\gamma_6}+e^{-K\omega\gamma_5})(1-e^{-K\omega^2 n})}{\omega^3\sqrt{1+\omega^2}}d\omega\right\} \qquad \text{(A8)}$$

with the notations;

$u_1=|x|/(z+\nu)$ $\quad u_2=|x|/|z-\nu|$ $\quad v_1=|x|/(z+n)$ $\quad v_2=|x|/|z-n|$ $\quad v_3=|x|/z$

$e_1=|x|+\omega(z+\nu)$ $\quad e_2=|x|-w(z+\nu)$ $\quad e_3=|x|+\omega|z-\nu|$ $\quad e_4=|x|-\omega|z-\nu|$

$\gamma_1=|x|+\omega(z+n)$ $\quad \gamma_2=|x|-\omega(z+n)$ $\quad \gamma_3=|x|+\omega|z-n|$ $\quad \gamma_4=|x|-\omega|z-n|$

$\gamma_5=|x|+\omega z$ $\quad \gamma_6=|x|-\omega z$

As $|x|\to 0$, the value of this double integral vanishes when $z\ge n$ and diverges as $\frac{\pi}{2K^2}(n-z)\lim_{\omega\to 0}\ln\omega$ when $0\le z<n$. It is to be noted that a logarithmic singularity exists in this latter case.